Effects of Cyclic and Post-cyclic Loading on Lateral Response of Flexible Piles Embedded in Dry Sand

Roozbeh Owji[1] · Ghassem Habibagahi[1] · Mehdi Veiskarami[1]

Abstract

This study aims to investigate the response of flexible piles in the course of cyclic and post-cyclic lateral loadings for different loading scenarios including cyclic loading pattern, loading frequency, and also amplitude. For this purpose, an experimental program has been organized and a series of tests were conducted on a model pile embedded in dry sand. Experimental p–y curves derived from bending moment profiles for different loading patterns, namely symmetric two-way, asymmetric two-way, full one-way, and one-way patterns without complete unloading were studied. The results indicate that the stiffness is highly dependent on the cyclic loading pattern, and the two-way cyclic loading was found to increase the lateral force and soil stiffness more than any other factor. Also, compared to the monotonic loading, the residual force induced by one-way loading and one-way loading without complete unloading causes the lateral bearing capacity to decrease significantly. In addition, the post-cyclic load–displacement response of the pile was found to be influenced by the number of cycles, loading amplitude, and soil density index. Finally, a comparative study revealed that predictions made by the API code for the lateral resistance of flexible piles embedded in dry sand underestimate the p–y curves obtained from experimental observation.

Keywords Cyclic loading · Flexible pile · Lateral loading · p–y curve · Post-cyclic

1 Introduction

Pile foundations supporting offshore and onshore structures including high-rise buildings, heavy structures, wind turbines, and transmission towers are often subjected to cyclic lateral loads induced by earthquakes, winds, and waves [1]. These repeated loads cause the soil around the pile to soften, followed by a progressive degradation in pile capacity [2]. The differences between the monotonic and cyclic loading lead to changes in soil reaction, lateral deflection along the pile, and the ultimate lateral capacity of the pile. The lateral capacity is usually considered as the main factor in dimensioning the piles [3]. The lateral

behavior of piles is often investigated using p–y curves in which the soil medium is represented as a series of elastic springs according to the Winkler beam model [4]. The p–y curves are nonlinear characteristic curves that relate the soil reaction to the lateral deflection of a pile with discrete springs. The API p–y curves [5], based on the work of Reese et al. [6], is the most widely used approach for predicting the response of the pile–soil system for monotonic and cyclic loading. API p–y curves were derived from field tests of flexible piles. The seamless steel pipe with dimeter of 610 mm and wall thickness of 9.5 mm was used as pile. The embedded length of pile was 21 m and the soil varied from clean fine sand to silty fine sand with high relative density. This method has limitations, p–y curves are independent of the cyclic loading pattern, loading frequency, number of cycles, and the amplitude. For cohesionless soils, API p–y curves account for the influence of the cyclic loading with a simplified approach that the ultimate soil resistance is reduced by an empirical factor (i.e., 0.9). Cyclic lateral loads based on the direction applied to the piles are categorized into one way and two

✉ Mehdi Veiskarami
  mveiskarami@gmail.com; mveiskarami@shirazu.ac.ir

  Roozbeh Owji
  roozbeh_73@yahoo.com

  Ghassem Habibagahi
  habibg@shirazu.ac.ir

1 School of Engineering, Shiraz University, Shiraz, Iran

way. Two-way cyclic loads can be symmetric or asymmetric based on the maximum and minimum values of the cyclic loading [7]. For instance, piles used for supporting wind turbines are probably subjected to both one-way and two-way cyclic loads. In recent years, various studies have been conducted to improve the prediction of pile behavior under lateral cyclic loading. Long and Vanneste investigated the influence of cyclic loading on piles installed in sandy soil [8]. They indicated that stiffness reduction during cyclic loading depends on soil density, pile installation method, and load ratio. Besides, they concluded that stiffness reduction caused by one-way cyclic loading is greater than two-way loading. LeBlanc et al. performed a series of cyclic loading tests on the small-scale rigid pile in sand [9]. In contrast to the API code, it was found that stiffness always increases with the number of cycles for both one-way and two-way loading tests and this increase is independent of relative density. Frick and Achmus investigated the influence of cyclic loading ratio on the lateral response of a rigid pile in sand [10]. They found that the maximum accumulated pile displacements occur in the case of an asymmetric two-way loading during the first 100 loading cycles. Darvishi Alamouti et al. performed a series of lateral loading tests on rigid piles in centrifuge [11]. Results showed that the maximum changes in the stiffness are associated with the first ten load cycles. Both increasing and decreasing trends of the stiffness are observed for the two-way loading pattern, whereas the increase in the stiffness is not observed in one-way loading. Arshad and O'Kelly showed that the accumulated rotation of a rigid pile under asymmetric two-way loading is higher than a symmetric two-way loading and the influence of the frequency on the rotation of the pile is negligible [12]. Hong et al. examined the influence of the one-way cyclic loading on the behavior of semi-rigid pile in soft clay [13]. At the last cycle of loading, plastic displacement of pile head was approximately 90% of the total displacement and with an increasing number of cycles, behavior of pile changed from flexible to rigid. Wang et al. conducted a series of field tests on semi-rigid piles installed in soft clay [14]. Results indicated that the stiffness reduction for pile undergoing two-way cyclic loading is higher than the pile subjected to one-way loading, while the cumulative residual deflection is higher for a one-way cyclic loading.

Some uncertainty exists in the previous studies with respect to variation in the stiffness of the soil surrounding the pile under cyclic loading; both increases and decreases of the stiffness were reported for two-way and one-way loadings. Although the direction of the cyclic loading is found to considerably affect the cyclic behavior of piles, a comparative study among the loading pattern and direction in a comprehensive single study has not been given special attention. The interaction between the soil and the pile

under lateral loading is governed by the relative stiffness of the pile–soil system [15]. In addition, most of the previous research has mainly focused on the behavior of rigid piles and little attention was paid to the influences of the cyclic loading on flexible piles.

The main motivation for this paper was to examine the interaction between the flexible pile and surrounding soil under different lateral cyclic loading directions including, symmetric two-way, asymmetric two-way, one-way, and one-way conditions without complete unloading. Moreover, the effects of loading frequency and cyclic amplitude on the changes in the secant stiffness and lateral force were also investigated. The ultimate lateral capacity of pile is highly influenced by changes in the pile–soil system. Therefore, it is important to investigate the ultimate lateral capacity caused by the cyclic loading effects. However, to the best of our knowledge, there have been no comprehensive studies to consider this important issue. For this purpose, a series of post-cyclic loading tests were conducted on model piles. All of the tests were conducted at the advanced soil mechanics laboratory of Shiraz University. More importantly, bending moments calculated from direct readings of instruments located along the model pile were used to develop the experimental p–y curves, which was then compared with the conventional p–y curves presented by the API code.

2 Materials and Methods

2.1 Properties of Soil

For a clear understanding of the influence of cohesionless soil on the lateral performance of a pile, silica sand with the mean grain size of 0.18 mm was used in this research. Figure 1 shows the particle size distribution curve for this
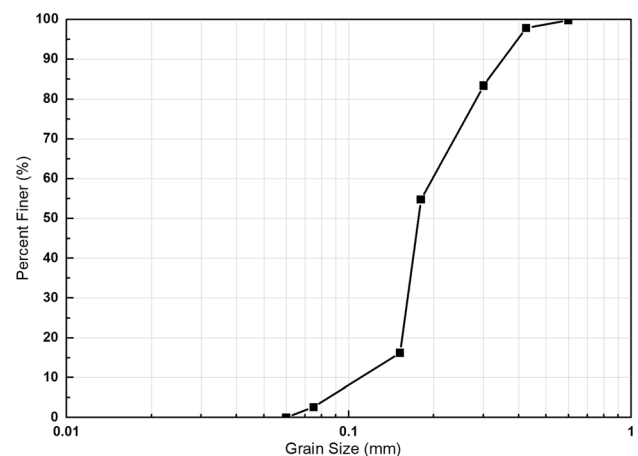

Fig. 1 Particle size distribution curve of the sand used in this study

sand, indicating that the coefficients of gradation (C_c) and uniformity (C_u) are 1.2 and 1.67, respectively. Based on the Unified Soil Classification System (USCS, ASTM D2487-00), the soil is classified as poorly graded sand (SP). The structural composition of the soil is between e_{min} = 0.68 and e_{max} = 0.92 and has a specific gravity of 2.65. The direct shear tests were conducted according to ASTM D3080 at a density index (i.e., relative density) of 40% with three different normal stresses, namely 50, 100, and 200 kPa, yielding an inter-particle friction angle and cohesion of 35° and 0, respectively.

2.2 Model Pile

Since full scale loading tests are quite expensive and time-consuming, small-scale tests are more commonly used and allow extensive parameters under a controlled condition in the laboratory to be investigated with higher accuracy. A variety of significant factors must also be considered when conducting pile loading tests at small scale, and these factors are explained here.

First, the model pile dimensions should be scaled down in a way that represents the actual full-scale behavior. Thus, the geometric dimensions of a prototype pile were scaled based on dimension analysis suggested by Wood et al. [16]:

$$\frac{E_m I_m}{E_n I_n} = \frac{1}{F^{4.5}}, \tag{1}$$

where F is the scale factor for length, $E_m I_m$ is the bending stiffness of the model pile, and $E_n I_n$ is the bending stiffness of the prototype pile. The geometrical scale factor considered in the model pile was about 22; details are depicted in Table 1.

A stainless steel tube with an outer diameter of 25 mm and wall thickness of 0.6 mm was used as model pile for performing lateral loading tests. The embedded length of 550 mm was enough to ensure the flexibility of the pile [17].

Table 1 Equivalent values for the model scale

| Physical quantity	Prototype pile Concrete	Model pile Steel
Embedded length of pile (m)	12	0.55
Pile diameter (m)	0.9	0.025
Elastic modulus of pile (GPa)	24	197
Bending stiffness of pile (kN m^2)	7.7×10^5	0.72
Elastic modulus of soil (MPa)	25	6.5
Relative stiffness	0.001	0.001

$$K_r = \frac{E_p I_p}{E_s L^4}, \tag{2}$$

where K_r is the relative stiffness of the pile–soil system and is lower than 0.0025 in the case of flexible pile, E_s is soil moduli, and L is embedded length of the pile. K_r was calculated to be 0.001 by assuming the soil moduli to be equal to 6.5 MPa. Therefore, we can ensure that the model pile behaves as a flexible pile under lateral loading. Since the scaling of the sand grains is impractical, criteria suggested by previous studies [18, 19] were employed to avoid particle size effect. If the minimum ratio of the model pile diameter (D_p) to the mean grain size of soil particles is typically beyond 50, or, more conservatively, 88, scale effects could be neglected. In the present experiment, this ratio was greater than 139 which is much higher than the conservative value of 88.

2.3 Test Box

A rectangular steel box with a length, width, and height of $600 \times 300 \times 900$ mm, respectively, was used for experimental model tests. The size of the steel box must be adequately large to avoid any boundary effects. The distance between the box sides and the model pile should be extended up to 8–$10D_p$ and 3–$4D_p$ along and perpendicular to the lateral loading direction, respectively [4, 20]. Moreover, the depth of the sand below the pile toe was maintained at a minimum of $6D_p$ to be able to mobilize the pile base stress. According to the above considerations, the friction between the soil particles and box walls can be disregarded. Besides, to overcome any lateral deflection of the box walls, steel plate with a thickness of 5 mm was chosen for the construction of box walls and Plexiglas with 15 mm thickness was used for the front side of the box. The interior sides of the soil box were graduated with 50 mm black and white plastic strips to facilitate accurate preparation of sand layers inside the box with the required density.

2.4 Cyclic loading System and Experimental Setup

In the present study, a new displacement-controlled device was designed and constructed to conduct cyclic and post-cyclic loading tests on pile with different loading directions at the advanced soil mechanics laboratory of Shiraz University. The loading device was installed at the upper edge of the soil box through a rigid frame and four bolts. A schematic form of the loading device can be envisioned in Fig. 2a, which includes a stepper motor, ball screw, ball nut, wagon, bearing support, and loading shaft. By rotating the stepper motor, the ball nut moves on the ball screw and
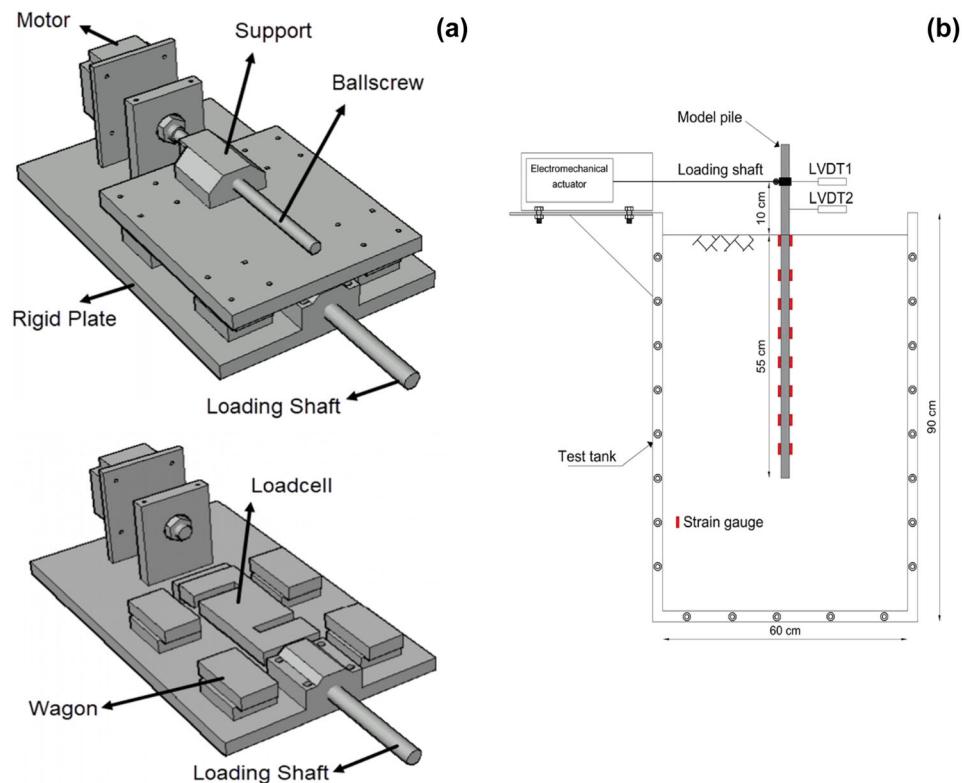
Fig. 2 a Expanded sketch of the loading device from top to bottom; **b** experimental setup and instrumentation

converts rotational motion to linear displacement. This linear motion is transferred to the loading shaft through a bearing plate and a wagon. The main function of the bearing support is to receive the load from the loading shaft and to support the ball screw axis. The loading shaft transfers the displacement to the aluminum clamp (i.e., the pile head) with a hinged connection to ensure free head condition. The force in the loading shaft is measured with a load cell installed between the two wagons that can measure a force up to 1.5 kN. The driver of the stepper motor was programmed to generate different types of loading including monotonic, cyclic, and post-cyclic loading. Horizontal pile head displacement was recorded continuously using two linear variable displacement transducers (LVDT) mounted at the top of pile as shown in Fig. 2b. One LVDT was directly connected to the load point and another one was placed 70 mm below the loading point. This arrangement allowed pile displacement at the ground surface to be measured, which was later used for the construction of p–y curves. The model pile was instrumented with eight pairs of strain gauges at 70 mm intervals along the outer surface of pile length with half-bridge arrangement to obtain bending moment profiles. The model pile was completely covered with heat shrink to prevent direct contact between sand and strain gauges. The output data

from the load cell, LVDTs, and strain gauges is recorded during all cyclic loading tests by a data logger system enhanced with computer software for data processing. To calibrate the strain gauge output, the model pile was tested as a cantilever beam and different weights were exerted to the end of the beam. The output data at each strain gauge location was calibrated with the calculated bending moment. More details of the loading conditions and sensor arrangements are shown in Fig. 3a.

In this research, the pre-installed method was considered to simulate non-displacement piles. It is noteworthy that under 1 g testing conditions, the effect of driving is negligible for model piles installed in medium dense sand [21]. For this purpose, the box was first filled with sand to achieve a location of the pile toe, afterward, the pile was placed at the center of box and was fixed to the loading shaft to be kept vertically on the soil bed (Fig. 3b). The dry sand was then carefully compacted with a tamping hammer in marked layers until desired relative density was obtained. In addition to monitoring the thickness of the soil layer, the required soil mass for each layer was weighed. When the appropriate embedded length of the pile was achieved, the soil surface was leveled to provide a flat surface. For the present research, density indices of 40%
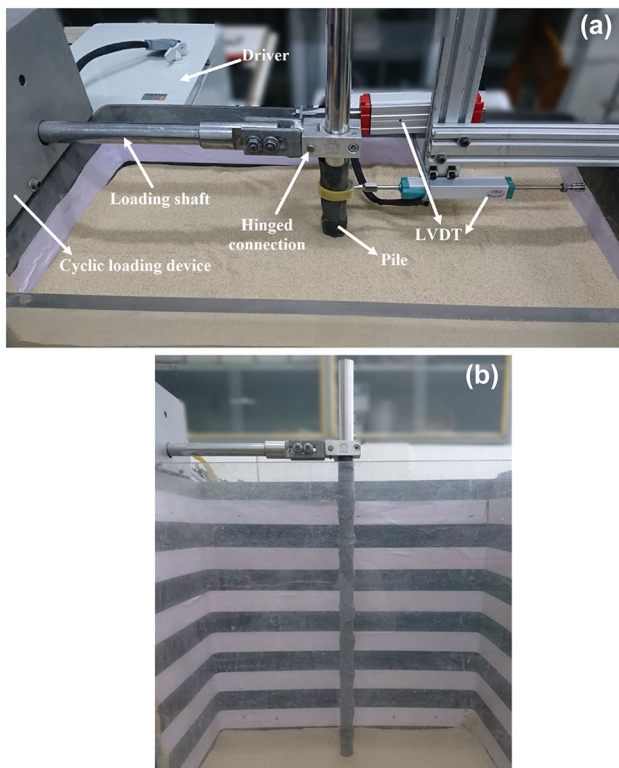
Fig. 3 Details of the experimental setup: **a** arrangement of the pile loading test; **b** view of the pile installation

and 65% corresponding to a dry unit weight of 14.25 and 14.73 kN/m^3 were considered.

2.5 Construction of p–y Curves

The relationship between soil resistance and lateral deflection along the pile is illustrated by p–y curves which can be obtained from bending moment profiles. Discrete points of the experimental moment were expressed by the polynomial fitting method to create smooth continuous curve. This allows the numerical differentiation and integration of the moment curve to be simplified. In the present study, the fifth-order polynomial equation [22] with an exponent of 2.5 instead of 2 was used to achieve the best estimate of experimental data. This slight modification in the exponential power was to make the soil reaction at the soil surface equal to zero.

$$M(z) = a_0 + a_1z + a_2z^{2.5} + a_3z^3 + a_4z^4 + a_5z^5, \tag{3}$$

where $M(z)$ is the bending moment fitted equation, and a_0, a_1, a_2, a_3, a_4, and a_5 are coefficients of the fifth-order polynomial determined with the least square method. The lateral soil reaction is obtained by taking derivatives of the

bending moment profile two times, with respect to the depth as shown in Eq. (4). Conversely, deflection can be derived with the double integration of the pile curvature $\left(\frac{M}{\text{EI}}\right)$ according to depth as follows:

$$p = -\frac{\mathrm{d}^2M}{\mathrm{d}z^2}, \tag{4}$$

$$y = \int\left(\int \phi\,\mathrm{d}z\right)\mathrm{d}z = \int\left(\int \frac{M}{\text{EI}}\,\mathrm{d}z\right)\mathrm{d}z, \tag{5}$$

where ϕ is the curvature of the pile, EI is the flexural modulus of pile, p is the lateral soil reaction per unit length of pile, and y is the lateral deflection along the pile. According to soil reaction (p), and lateral deflection (y), p–y curves were obtained.

2.6 Experimental Program

Three types of lateral loading including monotonic, cyclic, and post-cyclic were performed on model pile. Post-cyclic loading is defined as monotonic loading at the end of cyclic loading test. All loading tests conducted in the present study were under a displacement-controlled mode and the lateral load was introduced to the pile head at a height of 100 mm above the sand surface to simulate the influence of moments imposed at the ground surface. To measure the ultimate lateral capacity of the pile, a monotonic loading was conducted until the pile head displacement reached 20% of the pile diameter, marking the onset of failure [23]. Afterward, the pile was subjected to unloading until the force measured by the load cell returned to zero. Various cyclic loading directions, namely one-way, one-way without complete unloading, symmetric two-way, and asymmetric two-way directions over the duration of 100 cycles of loading were investigated. For the sake of evaluating the loading frequency, a series of frequencies of 0.05, 0.1, and 0.2 Hz were assumed in cyclic loading tests. The main reason behind such a choice was the common range of frequencies in wind turbines (as well as other such structures) which is around 0.1 Hz [24]. Moreover, three displacement amplitudes including $0.08D_p$, $0.12D_p$, and $0.16D_p$ were investigated. The details of the test program and load characteristics are given in Table 2. It is important to note that owing to the nature of the cyclic loads (with fairly low frequency) the inertial force, originated from the mass of the pile and small soil attached to the pile and moving together with the pile, is insignificant compared to the force, applied to the pile head. Therefore, the inertial force is negligible and the results are applicable to cases with similar loading condition.
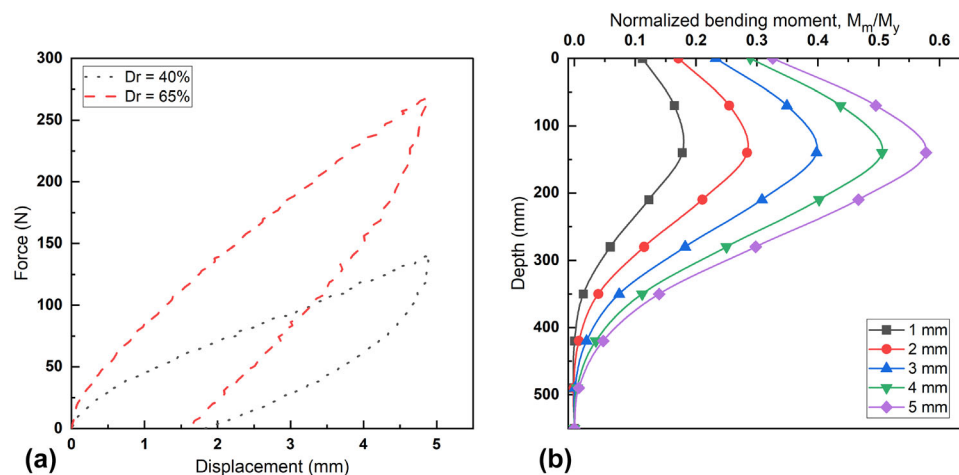
Table 2 Summary of the test program

Test number	Loading type	D_r (%)	y_{max} (mm)	y_{min} (mm)	Frequency (Hz)
1	Monotonic	40	–	–	–
2	Cyclic, post-cyclic	40	3	– 3	0.1
3	Cyclic, post-cyclic	40	3	– 2	0.1
4	Cyclic, post-cyclic	40	3	0	0.1
5	Cyclic, post-cyclic	40	3	2	0.1
6	Monotonic	65	–	–	–
7	Cyclic	65	3	– 3	0.1
8	Cyclic	65	3	– 2	0.1
9	Cyclic	65	3	0	0.1
10	Cyclic	65	3	2	0.1
11	Cyclic, post-cyclic	40	3	– 3	0.2
12	Cyclic, post-cyclic	40	3	– 3	0.05
13	Cyclic, post-cyclic	40	4	0	0.1
14	Cyclic, post-cyclic	40	2	0	0.1

3 Results and Discussion

3.1 Monotonic Test Results

Load–displacement responses of a pile subjected to monotonic loading is represented in Fig. 4a. For both density indices, the pile head forces increase approximately linearly with applied displacement. This indicates that the pile–soil system is in a quasi-elastic region. Increasing the density index from medium dense to dense leads to an increase in the lateral capacity by 107%, showing a significant change. Loading–unloading tests generate plastic displacements at pile head with the same value observed for both density indices; approximately 70% of the pile head displacement was recovered. Figure 4b shows the distribution of the bending moment along the pile during a monotonic loading for a density index of 65%. From the general shape of the curves, it can be concluded that the number of strain gauges were enough. The measured bending moment (M_m) was normalized by the so-called yielding moment (M_y) determined from material properties of the pile. The maximum bending moment at any displacement level occurs approximately $6D_p$ below the ground surface and gradually increases with the load magnitude. As shown in Fig. 4b, it is clear that at the ultimate state (i.e., at a horizontal displacement of about $0.2D_p$) defined by Broms [23], the flexural capacity of the pile has not been reached; therefore, a structural failure mode of the pile would not occur. It is noteworthy that the flexural capacity governs the design of flexible piles and the pile fails before the surrounding soil. In the existing literature, there is no standard criterion for the definition of the lateral capacity of flexible piles. However, in this study, Broms method was used for the definition of the lateral bearing capacity of a pile [23].

3.2 Cyclic Test Results

The influence of the cyclic loading on pile–soil stiffness variation was investigated by measuring the cyclic secant stiffness defined as the slope of the line drawn between the end points on the load–displacement curve in each cycle of the loading as demonstrated in Fig. 5. To better understand
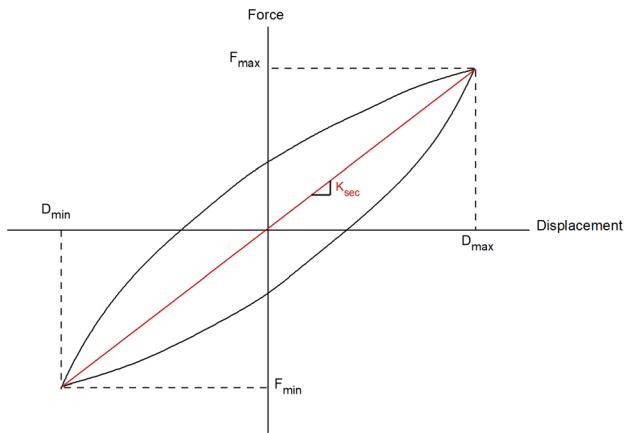

Fig. 4 Monotonic loading test results: **a** load–displacement response; **b** normalized bending moment profiles for different displacement levels at density index of 65%

Fig. 5 Cyclic secant stiffness definition for a pile–soil system

the lateral stiffness changes, the secant stiffness of the pile–soil system at each cycle was normalized to the secant stiffness of the first cycle.

Figure 6 shows the effect of cyclic loading direction in dry sand with a density index of 40%. For two-way cyclic loading, the stiffness shows a gradual increase with the number of cycles and the difference between the symmetric and asymmetric loading conditions is marginal (Fig. 6a). For one-way cyclic loading, the stiffness decreases within the first ten load cycles, followed by a steady increase in the stiffness. For one-way loads without complete unloading, in contrast to the other cases, an increase in the stiffness is not observed and becomes constant after ten cycles of loading. Figure 6b represents the variation of the maximum force at the pile head during the 100 cycles of loading. As expected, the lateral capacity of the pile increases under two-way cyclic loading, approximately 25% increase in the lateral force occurs after 100 cycles. This improvement in the lateral capacity is associated with local densification in the vicinity of the pile during the cyclic loading leading as sand particles move downward, which marks subsidence in the soil surface. Similar observations were also reported in previous studies [10, 25]. For one-way loading, the lateral head force decreases during the first ten load cycles and then becomes approximately constant at a value of 90 N for the remaining cycles. It can be seen that one-way loads without complete unloading result in a significant reduction in the lateral capacity of the pile.

All the aforementioned findings may suggest that the lateral pile head force under cyclic loading can either increase or decrease depending on the cyclic loading direction or pattern. The reason for increasing the lateral capacity under two-way loading compared to one-way loading may be due to the fact that the two-way loading includes a reversal in the loading direction and hence, it densifies the surrounding sand in both directions. However,
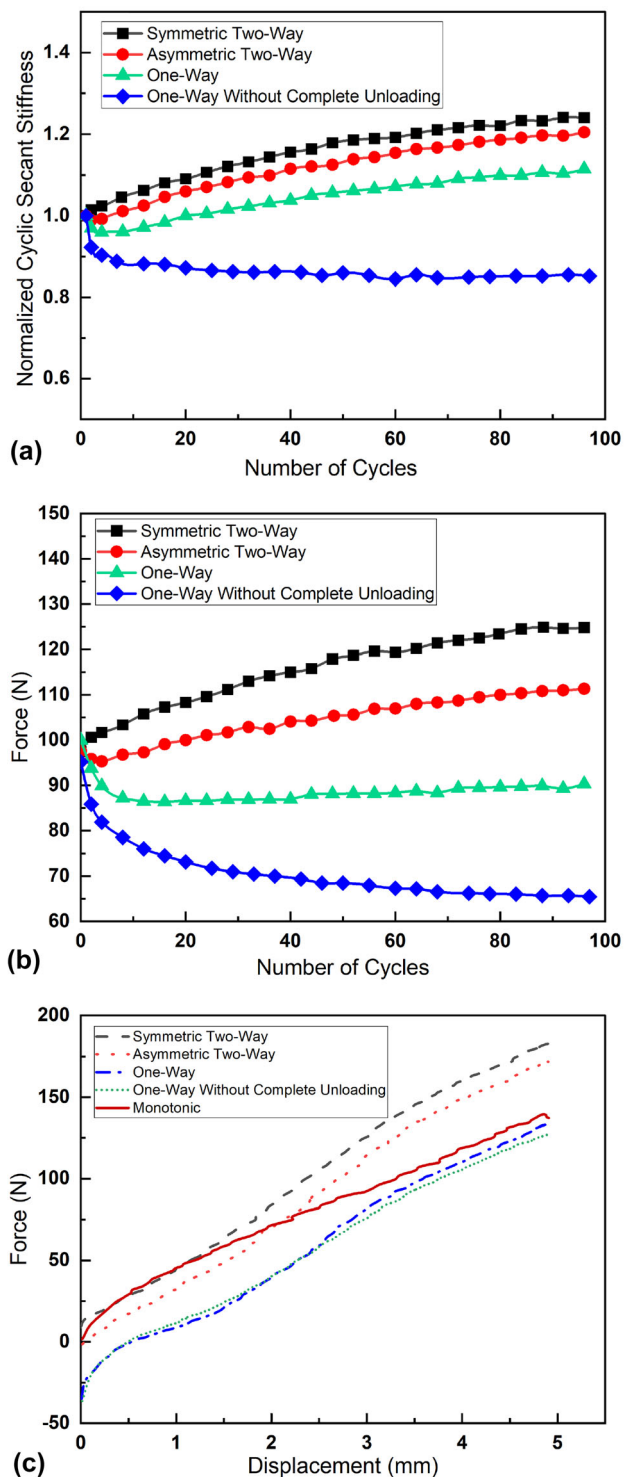

Fig. 6 Cyclic loading results for density index of 40%: **a** variation of cyclic secant stiffness; **b** variation of maximum pile head force; **c** post-cyclic load–displacement response

under one-way loads, an increase in the stiffness is due to the accumulation of the residual force at the pile head.

The influence of the cyclic loading direction on the post-cyclic response of the pile is depicted in Fig. 6c. The

residual force that was induced by cyclic loading in the case of one-way and one-way loadings without complete unloading can be seen in the same figure. For the case of two-way loading, it is obvious that with further increasing the displacement, the lateral force increases to a level higher than that of monotonic loading. These results confirm that the two-way cyclic loading has a positive influence on the ultimate lateral capacity of a pile installed in dry sand. A similar response is observed for both one-way loading and one-way loading without complete unloading, converging to the monotonic loading as the loading progresses. In addition, although one-way loading without complete unloading appears to have some negative effects on stiffness and lateral force, the ultimate lateral capacity of the pile does not change significantly.

Cyclic loading test results for soil with density index of 65% is shown in Fig. 7. Variation of the force and secant stiffness have similar trend with density index of 40% but in the case of a two-way loading, the rate of the increase in the lateral force and stiffness for density index of 40% is higher than that of density index of 65%.

3.3 Locked-In Bending Moment Profile

Bending moment profiles of pile during cyclic loading when the pile head displacement (for displacement-controlled loading) is zero are defined as "locked-in moment" [26]. This can be attributed to the locking in the soil stress and the residual force remaining in pile head. Figure 8a shows the locked-in moment for different cyclic loading directions at the end of cyclic loading tests. It is clear that locked-in moment developed under one-way loads without complete unloading and one-way loading tests are significantly higher than two-way loading tests. Although two-way loading causes the maximum lateral force, a marginal locked-in moment is observed for piles undergoing symmetric two-way loading. The reason for this may be that

reversed component of a symmetric two-way cyclic loading decreases or destroys locked-in soil stress and consequently reduces the locked-in bending moment [14]. A locked-in moment after 1st, 50th, and 100th cycle of one-way loading is depicted in Fig. 8b. The locked-in moment is affected by the number of cycles and at 100th cycle of loading, the maximum locked-in moment increased by up to 90%.

3.4 Accumulation of Residual Force

Figure 9 shows accumulated residual force at the pile head during 100 cycles of one-way loading. It can be seen that residual force increases with the number of cycles, consistent with the increasing locked-in moment. For both density indices, the rate of accumulation is rapid during the first few cycles and then residual force gradually increases at constant rate. Residual force is highly influenced by density index, as the density index increases from 40 to 65%, the accumulated residual force also increases by approximately 50%.

3.5 Effect of Loading Frequency

Figure 10 indicates the effect of loading frequency on the stiffness and pile head force during a symmetric two-way cyclic loading. For a frequency of 0.2 Hz, the rate of increase in the stiffness is considerably higher than that of frequencies of 0.1 Hz and 0.05 Hz, in which the stiffness of the pile–soil system increases by 40% after 100 cycles of loading. This implies that the densification around the pile is affected by the frequency and the effect of the frequency on the pile response may depend on the soil type and density index. Variation of the maximum pile force over time is shown in Fig. 10b. As expected, increasing the loading frequency from 0.1 to 0.2 Hz had a significant influence on the enhancement of the lateral capacity in
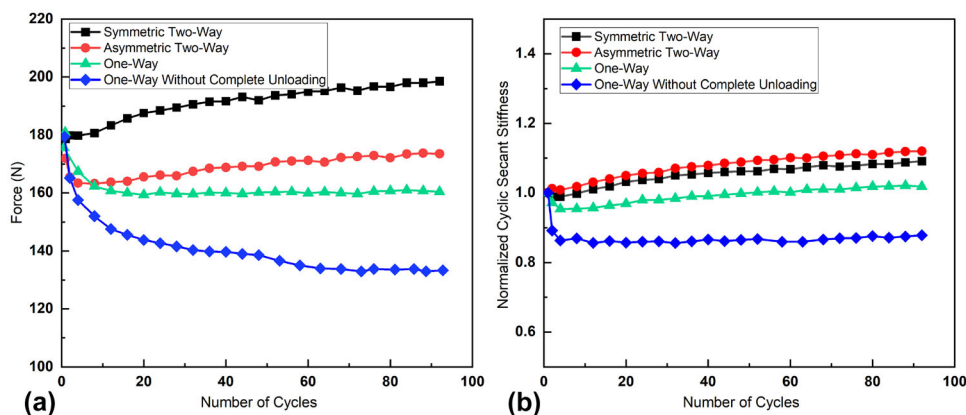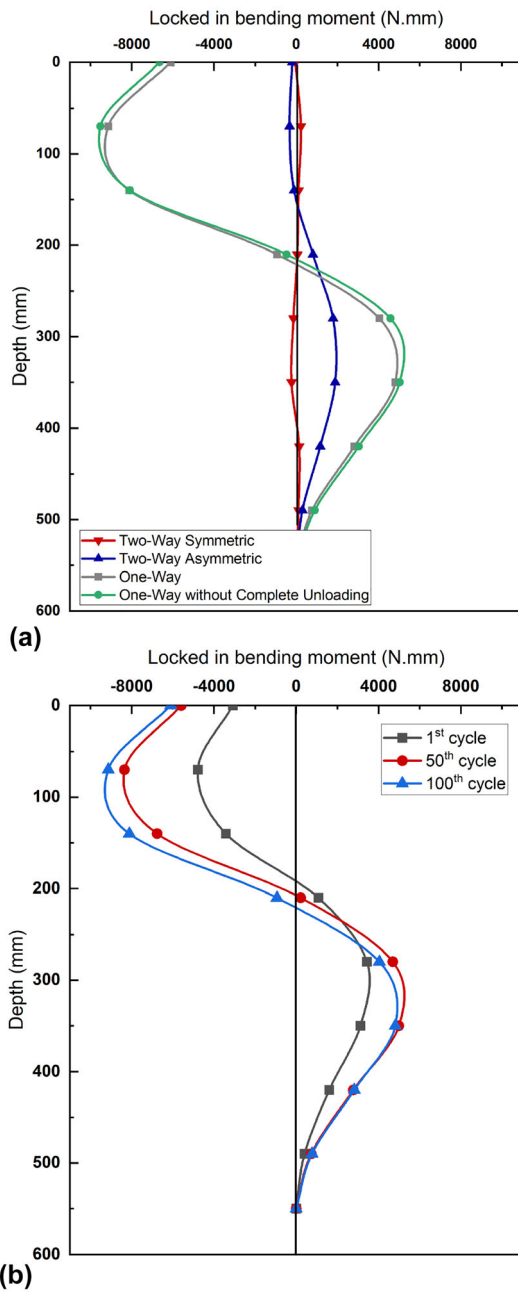

Fig. 7 Cyclic loading results for density index of 65%: **a** variation of maximum pile head force; **b** variation of cyclic secant stiffness
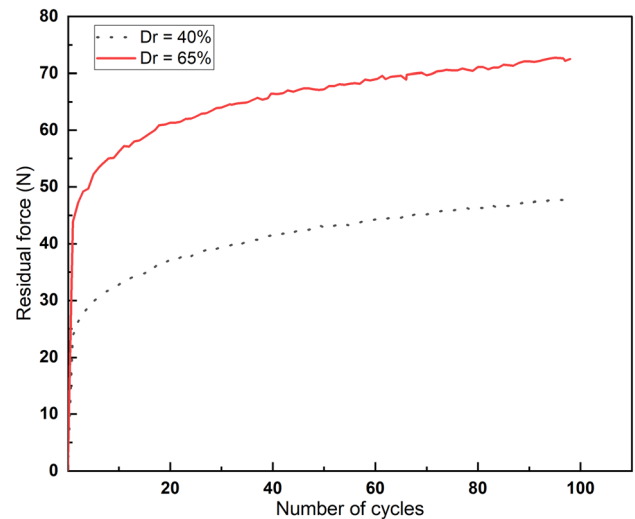
(a)

(b)

Fig. 8 Distribution of locked-in moment along the pile at the density index of 65%: **a** locked-in moment at the end of cyclic loading test; **b** locked-in moment at the 1st, 50th, and 100th cycle of one-way loading
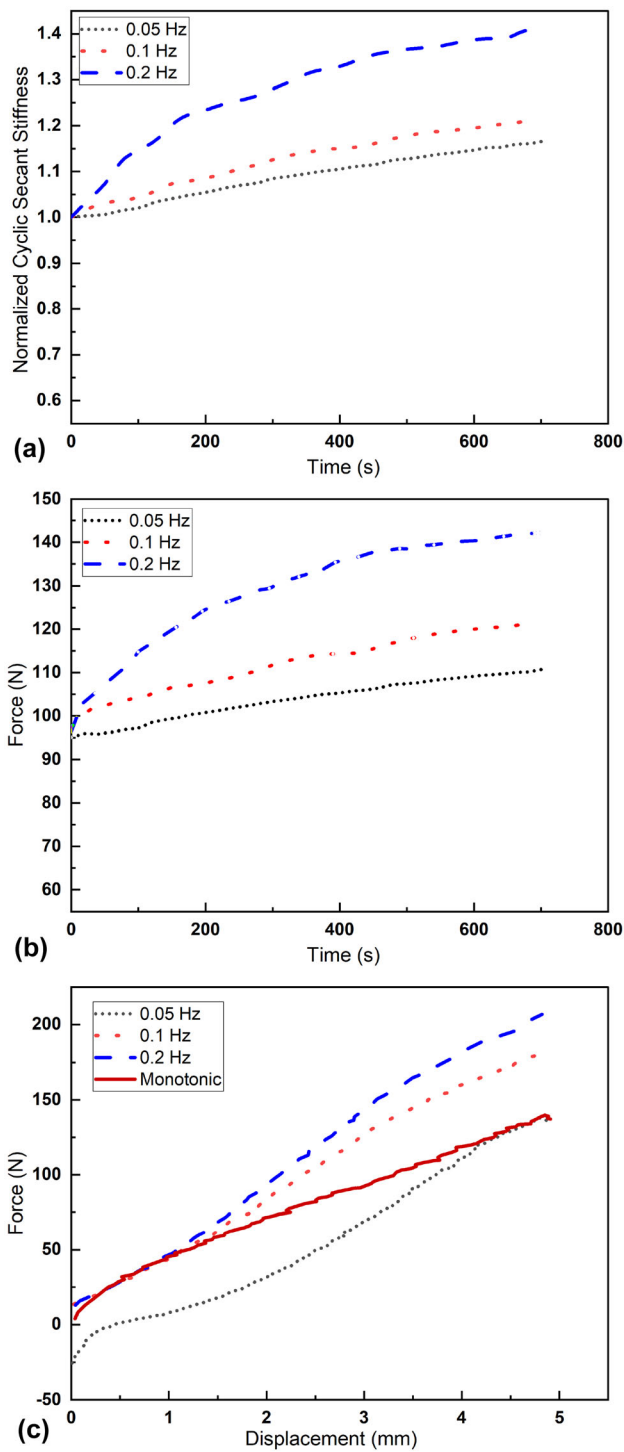

Fig. 9 Accumulation of residual force during one-way cyclic loading test

diameter. Meanwhile, the lateral force increases nonlinearly with increasing the displacement until it reaches an ultimate state in accordance with the monotonic bearing capacity. This implies that the residual force due to the cyclic loading has a significant influence on the lateral behavior of the pile, whereas it cannot affect the ultimate lateral resistance compared to a monotonic loading. It can be observed that the tests carried out with loading frequencies of 0.1 Hz and 0.2 Hz exhibit higher lateral capacity than in a monotonic loading test. This is mainly attributed to the densification and further increase in the soil stiffness around the pile during a two-way cyclic loading.
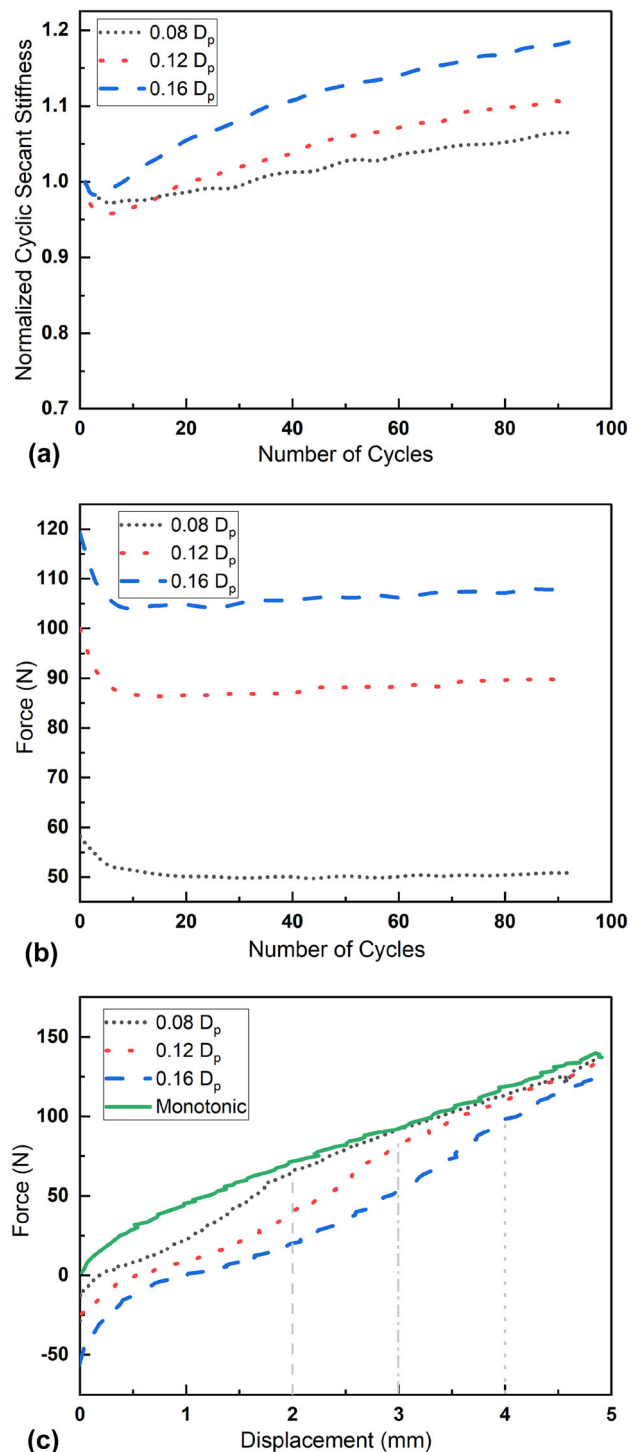
3.6 Effect of Amplitude

Figure 11 shows the results of cyclic loading tests at different cyclic displacement amplitudes under one-way cyclic loading. In all cases, cyclic secant stiffness decreases in the first few cycles and then gradually increases with increasing the number of load cycles. The rate of increase in stiffness shows an increasing tendency as the displacement increases. Variation of the pile head force for different displacement amplitudes is shown in Fig. 11b. The cyclic lateral capacity of the pile decreases during the first ten cycles and thereafter, a constant force level is reached indicating that the accumulation of residual force at the pile head is the main reason for the increase in the secant stiffness in one-way cyclic loading. Larger cyclic displacement amplitude leads to an increase of lateral force and this increase is not proportional to the increase in the amplitude; for example, an increase of the amplitudes from $0.08D_p$ to $0.12D_p$ and from $0.12D_p$ to $0.16D_p$ result in 80%

which pile head force increases by 40% at the last cycle of the loading, while increasing the frequency from 0.05 to 0.1 Hz results in an increase of the pile head force by 20%.

The effect of the frequency on the load–displacement response of the pile under the post-cyclic loading is depicted in Fig. 10c. Cyclic loading with the frequency of 0.05 Hz causes residual force in the reversed direction and leads to a reduction in the lateral capacity in the displacement range of 0–4 mm corresponding to 0.16 pile

Fig. 10 Effect of loading frequency on lateral pile response for two-way symmetric loading: **a** variation of cyclic secant stiffness; **b** variation of maximum pile head force; **c** post-cyclic load–displacement response

Fig. 11 Effect of cyclic load amplitude on lateral pile response for one-way loading: **a** variation of cyclic secant stiffness; **b** variation of maximum pile head force; **c** post-cyclic load–displacement response

and 20% increases in the lateral force, respectively. Figure 11c shows the influence of different cyclic displacement amplitudes on the load–displacement response under post-cyclic loading. The magnitude of the residual force

induced by the cyclic loading is affected by the cyclic amplitude and at larger amplitudes, higher residual forces are observed. As shown in Fig. 11c, these residual forces reduce the lateral capacity of the pile in the displacement

range corresponding to the cyclic displacement amplitude; for example, under cyclic amplitude of $0.12D_p$, the post-cyclic behavior of the pile tends to converge to that of the monotonic loading after displacements of about $0.12D_p$. These results highlight the influence of the cyclic amplitude on the pile behavior in post-cyclic loadings.

## 3.7 Interpretation of Soil Reaction and Deformation

Soil reaction and deformation obtained from the bending moment profile are presented in this section. Figure 12 shows lateral deflection and soil reaction along the pile for density index of 40% and 65% under monotonic loading. Figure 12a confirms that the pile behaves as a flexible pile for both density indices and the point of zero deflection initiates from the depth of $12D_p$. This implies that the depth from 0 to $12D_p$ below the soil surface plays an important role in the behavior and lateral capacity of the pile. The maximum soil reaction occurs at a depth of $4D_p$ and this magnitude for the sand at dense state is 22 times larger than that of the medium state. This means that the soil will reach an ultimate resistance at the upper portion of the pile. A comparison of the soil reaction profiles between monotonic and cyclic loading (at 100th cycle of loading) for a density index of 65% is depicted in Fig. 12c. The key finding is that the cyclic loading of the pile affects only the upper layers of the soil. Under two-way loading, hardening behavior is observed while under one-way loading and one-way loading without complete unloading, degradation behavior can be visualized. Moreover, the depth of the maximum soil reaction did not change with cyclic loading directions.

The experimental p–y relationship for both monotonic and cyclic loading is illustrated in Fig. 13. Similar non-linear trend with different ultimate resistance and stiffness is observed for all types of loading. A comparison of p–y curves between monotonic loading and those of cyclic loading represents that the two-way cyclic loading causes higher lateral soil resistance, whereas the pile undergoing one-way loading exhibits softer lateral response. The soil resistance mobilized around the pile under a two-way cyclic loading is always higher than that of one-way loading. Moreover, flattening representing the ultimate soil resistance is not observed for experimental p–y curves. For a density index of 65%, all experimental curves lie above the API curve at any displacement level and with increasing lateral deflection, show stiffer responses compared to API curve. For density index of 40%, the API curve overestimates the soil resistance of the pile undergoing one-way loads without complete unloading while it underestimates for other cases of loading. These results imply that p–y curves are highly dependent on the direction of cyclic loading which is not considered by the API code.
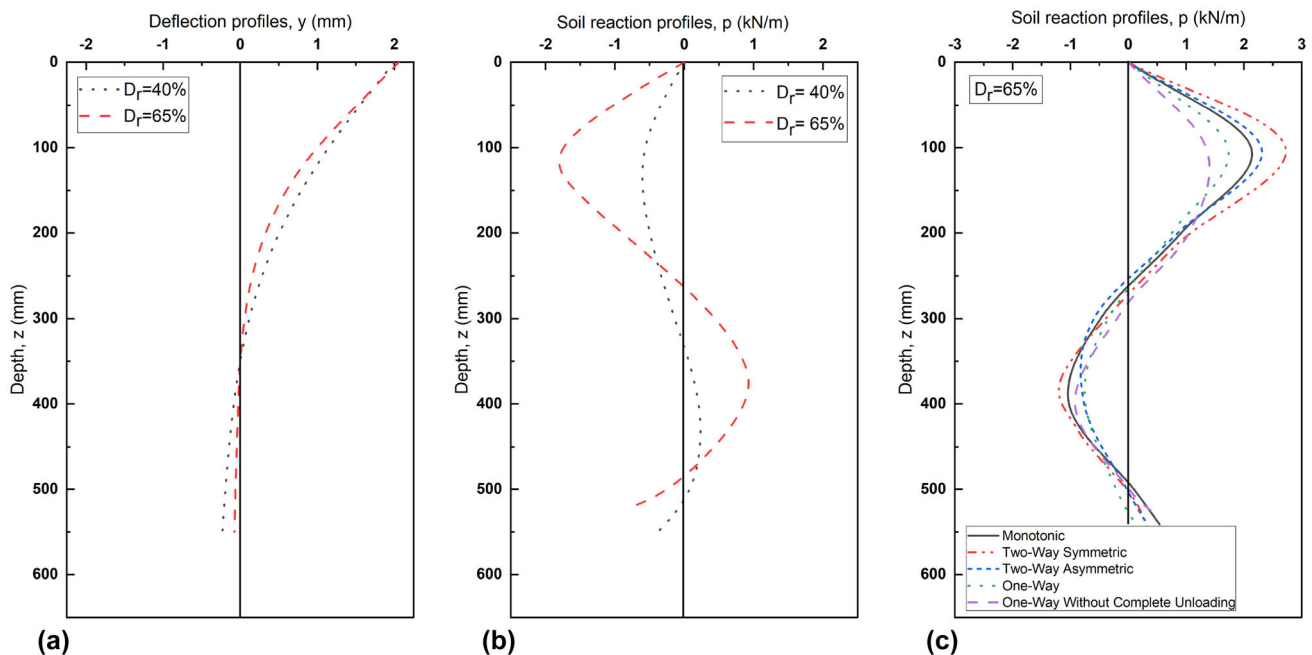
Fig. 12 Soil reaction and deflection obtained from bending moments: **a** lateral deflection profiles of pile under monotonic loading ($D_r = 40\%$ and 65%); **b** soil reaction profiles under monotonic loading ($D_r = 40\%$ and 65%); **c** soil reaction profiles at 100th cycle of loading (just for $D_r = 65\%$)
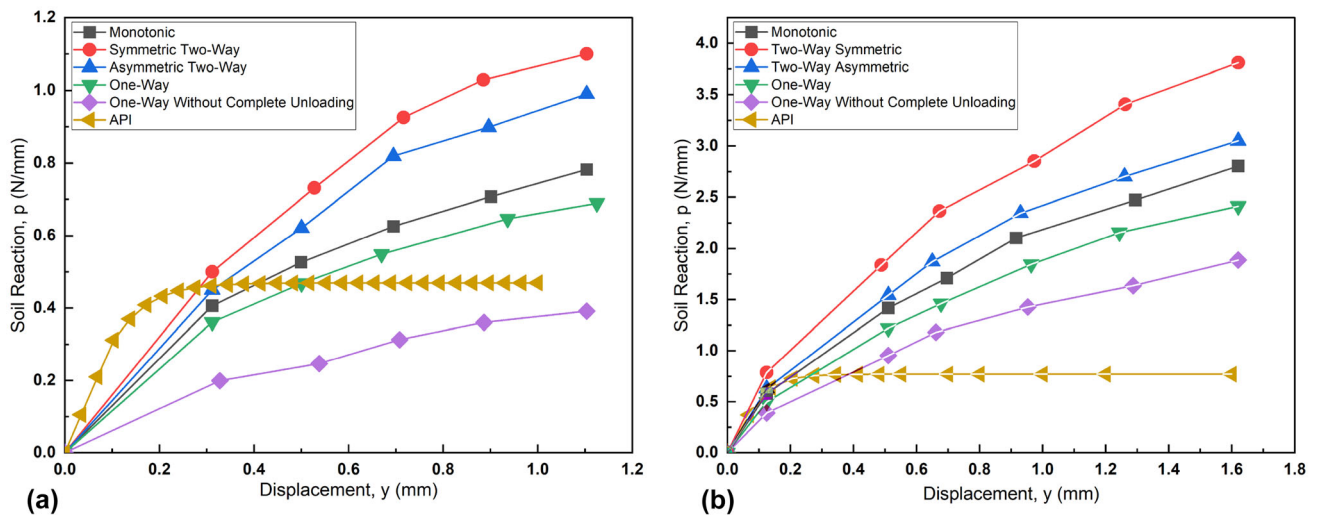
Fig. 13 Experimental p–y curves at depth of $4D_p$: **a** density index of 40%; **b** density index of 65%

4 Conclusions

The aim of this study was to investigate the response of flexible piles under lateral monotonic, cyclic, and post-cyclic loadings in dry dense and medium dense sands. A comprehensive set of cyclic loading tests was performed to evaluate the effect of the loading directions or pattern, frequency, number of cycles, and the loading amplitude on the variation of the lateral force and stiffness of the pile–soil system. Moreover, experimental cyclic and monotonic p–y curves obtained from bending moment profiles were compared. The following conclusions can be drawn from the results of the current study:

- Two-way cyclic loading resulted in an increase of the cyclic secant stiffness and lateral force for both density indices of 40% and 65%. The primary mechanism causing this response is the local densification of the sand around the pile. In contrast, under the one-way loading without complete unloading, the stiffness degradation was observed. Moreover, the cyclic secant stiffness under two-way loading was observed to increase with the loading frequency and larger ultimate lateral capacities were also obtained, compared to the monotonic loading condition.
- Compared to the monotonic loading, post two-way cyclic loading increased the ultimate lateral capacity of the pile, however, negligible change was observed under one-way loading condition. In addition, the residual force caused by the cyclic loading had a significant influence on the post-cyclic load–displacement behavior of the pile.
- In general, the p–y curves obtained from the test results of two-way loading condition indicated a stiffer response compared to the one-way loading. By

comparing the API p–y curve with the experimental curves, it can be concluded that the API code underestimates the ultimate lateral resistance of the flexible piles for both monotonic and cyclic loading. Therefore, the API code results in a conservative estimation for the lateral behavior of piles.

- Residual forces induced under one-way loading condition (with and without complete unloading) led to the development of locked-in moment along the pile length which increased with the number of load cycles. For example, maximum locked-in bending moment increased by 80% during 100 cycles of loading. Moreover, it was shown that the residual force was highly dependent on the cyclic displacement amplitudes and density indices.

Finally, it is important to mention that this study was conducted on scaled model piles. Therefore, research is encouraged to study the pile response using geotechnical centrifuge tests or actual field condition to further enrich and/or modify the obtained results; hence, this is still an open area for future research.

References

1. Basack S (2015) Design recommendations for pile subjected to cyclic load. Mar Georesour Geotechnol 33(4):356–360. https://doi.org/10.1080/1064119X.2013.778378
2. Basack S, Nimbalkar S (2018) Measured and predicted response of pile groups in soft clay subjected to cyclic lateral loading. Int J Geomech 18(7):04018073. https://doi.org/10.1061/(ASCE)GM.1943-5622.0001188

3. Langer JA et al (1984) Laterally loaded deep foundations: analysis and performance: a symposium. ASTM In. https://doi.org/10.1520/STP835-EB

4. Matlock H (1970) Correlation for design of laterally loaded piles in soft clay. In: Offshore technology conference. OnePetro. https://doi.org/10.4043/1204-MS

5. Api R (2000) Recommended practice for planning, designing and constructing fixed offshore platforms-working stress design. API RP A 2

6. Reese LC, Cox WR, Koop FD (1974) Analysis of laterally loaded piles in sand. In: Offshore technology conference. OnePetro. https://doi.org/10.4043/2080-MS

7. Rao SN, Rao KM (1993) Behaviour of rigid piles in marine clays under lateral cyclic loading. Ocean Eng 20(3):281–293. https://doi.org/10.1016/0029-8018(93)90025-D

8. Long J, Vanneste G (1994) Effects of cyclic lateral loads on piles in sand. J Geotech Eng 120(1):225–244. https://doi.org/10.1061/(ASCE)0733-9410(1994)120:1(225)

9. LeBlanc C, Houlsby G, Byrne B (2010) Response of stiff piles in sand to long-term cyclic lateral loading. Géotechnique 60(2):79–90. https://doi.org/10.1680/geot.7.00196

10. Frick D, Achmus M (2020) An experimental study on the parameters affecting the cyclic lateral response of monopiles for offshore wind turbines in sand. Soils Found 60(6):1570–1587. https://doi.org/10.1016/j.sandf.2020.10.004

11. Darvishi Alamouti S, Moradi M, Bahaari MR (2019) Centrifuge modelling of monopiles subjected to lateral loading. Sci Iran 26(6):3109–3124. https://doi.org/10.24200/sci.2018.20222

12. Arshad M, O'Kelly BC (2014) Development of a rig to study model pile behaviour under repeating lateral loads. Int J Phys Model Geotech 14(3):54–66. https://doi.org/10.1680/ijpmg.13.00015

13. Hong Y et al (2017) Cyclic lateral response and failure mechanisms of semi-rigid pile in soft clay: centrifuge tests and numerical modelling. Can Geotech J 54(6):806–824. https://doi.org/10.1139/cgj-2016-0356

14. He B, Wang L, Hong Y (2017) Field testing of one-way and two-way cyclic lateral responses of single and jet-grouting reinforced piles in soft clay. Acta Geotech 12(5):1021–1034. https://doi.org/10.1007/s11440-016-0515-z

15. Zhu B et al (2016) Centrifuge model tests on laterally loaded piles in sand. Int J Phys Model Geotech 16(4):160–172. https://doi.org/10.1680/jphmg.15.00023

16. Wood DM, Crewe A, Taylor C (2002) Shaking table testing of geotechnical models. Int J Phys Model Geotech 2(1):01–13. https://doi.org/10.1680/ijpmg.2002.020101

17. Poulos H (1982) Single pile response to laterally cyclic load. J Geotech Eng ASCE 108(GT-3):355–375. https://doi.org/10.1061/AJGEB6.0001255

18. Zhu B et al (2021) Centrifuge modeling of monotonic and cyclic lateral behavior of monopiles in sand. J Geotech Geoenviron Eng 147(8):04021058. https://doi.org/10.1061/(ASCE)GT.1943-5606.0002566

19. Klinkvort RT, Hededal O (2013) Lateral response of monopile supporting an offshore wind turbine. Proc Inst Civ Eng Geotech Eng 166(2):147–158. https://doi.org/10.1680/geng.12.00033

20. Khari M, Kassim KA, Adnan A (2013) An experimental study on pile spacing effects under lateral loading in sand. Sci World J 2013:1–18. https://doi.org/10.1155/2013/734292

21. Rathod D, Nigitha D, Krishnanunni K (2021) Experimental investigation of the behavior of monopile under asymmetric two-way cyclic lateral loads. Int J Geomech 21(3):06021001. https://doi.org/10.1061/(ASCE)GM.1943-5622.0001920

22. Wilson DW (1998) Soil-pile-superstructure interaction in liquefying sand and soft clay, vol 1998. Citeseer, Princeton. https://doi.org/10.5703/1288284314332

23. Broms BB (1964) Lateral resistance of piles in cohesionless soils. J Soil Mech Found Div 90(3):123–156. https://doi.org/10.1061/JSFEAQ.0000614

24. Abadie CN et al (2019) Rigid pile response to cyclic lateral loading: laboratory tests. Géotechnique 69(10):863–876. https://doi.org/10.1680/jgeot.16.P.325

25. Faresghoshooni A, Imam S, Mahmoodi A (2021) Model testing on the effects of section geometry and stiffness on the cyclic lateral behavior of piles in loose sand. Int J Civ Eng 19(5):563–581. https://doi.org/10.1007/s40999-020-00548-x

26. Kirkwood P, Haigh S (2014) Centrifuge testing of monopiles subject to cyclic lateral loading. In: Proceedings of the 8th international conference on physical modelling in geotechnics. Taylor & Francis Group, London, UK